



Climate change projections for the tropical Andes using a regional climate model: Temperature and precipitation simulations for the end of the 21st century

Rocío Urrutia^{1,2} and Mathias Vuille^{1,3}

Received 22 August 2008; revised 6 November 2008; accepted 18 November 2008; published 23 January 2009.

[1] High-elevation tropical mountain regions may be more strongly affected by future climate change than their surrounding lowlands. In the tropical Andes a significant increase in temperature and changes in precipitation patterns will likely affect size and distribution of glaciers and wetlands, ecosystem integrity, and water availability for human consumption, irrigation, and power production. However, detailed projections of future climate change in the tropical Andes are not yet available. Here we present first results for the end of the 21st century (2071–2100) using a regional climate model (RCM) based on two different emission scenarios (A2 and B2). The model adequately simulates the spatiotemporal variability of precipitation and temperature but displays a cool and wet bias, in particular along the eastern Andean slope during the wet season, December–February. Projections of changes in the 21st century indicate significant warming in the tropical Andes, which is enhanced at higher elevations and further amplified in the middle and upper troposphere. Temperature changes are spatially similar in both scenarios, but the amplitude is significantly higher in RCM-A2. The RCM-A2 scenario also shows a significant increase in interannual temperature variability, while it remains almost unchanged in RCM-B2 when compared to a 20th century control run. Changes in precipitation are spatially much less coherent, with both regions of increased and decreased precipitation across the Andes. These results provide a first attempt at quantifying future climate change in the tropical Andes and could serve as input for impact models to simulate anticipated changes in Andean glaciation, hydrology, and ecosystem integrity.

Citation: Urrutia, R., and M. Vuille (2009), Climate change projections for the tropical Andes using a regional climate model: Temperature and precipitation simulations for the end of the 21st century, *J. Geophys. Res.*, *114*, D02108, doi:10.1029/2008JD011021.

1. Introduction

[2] Mountain regions play a critical role for downstream water supply in the arid and semiarid regions of the tropics and subtropics, affecting millions of people [Viviroli *et al.*, 2007]. This is particularly true for the tropical Andes, which are relatively moist compared with the adjacent hyperarid coastal desert to the west. Much of the rain and snow falling in the tropical Andes is initially stored, either as ice in mountain glaciers or as water, retained in high-altitude tropical wetlands (“páramos”), before being gradually released over time [Buytaert *et al.*, 2006; Juen *et al.*, 2007; Vuille *et al.*, 2008a]. Glaciers and páramos therefore act as critical buffers against highly seasonal precipitation and provide water for domestic, agricultural or industrial

use during the dry season, when rainfall is low or absent. Yet climate change may soon lead to dramatic changes in Andean hydrology, with unknown consequences regarding the availability of water for human consumption, irrigation, mining, power generation and the social and cultural life of Aymara and Quechua cultures [Young and Lipton, 2006; Vergara *et al.*, 2007]. While changes in climate are already being observed [Vuille and Bradley, 2000; Vuille *et al.*, 2003] and glaciers are retreating throughout the tropical Andes [Ramirez *et al.*, 2001; Francou *et al.*, 2003, 2004; Jordan *et al.*, 2005; Mark and Seltzer, 2005; Ceballos *et al.*, 2006; Thompson *et al.*, 2006; Mark and McKenzie, 2007; Seimon *et al.*, 2007; Vuille *et al.*, 2008a] detailed assessments of how climate will change in the 21st century and how these changes will impact the environmental service provided by glaciers and wetlands are sorely missing. Here we take a first step in this direction by simulating different scenarios of future climate change in the tropical Andes as provided by the Intergovernmental Panel on Climate Change—Special Report on Emission Scenarios (IPCC-SRES) [Nakicenovic and Swart, 2000], using a high-resolution Regional Climate Model (RCM). Such high-resolution models, run over a limited domain have been successfully applied in studies of

¹Climate System Research Center, University of Massachusetts, Amherst, Massachusetts, USA.

²Now at Laboratorio de Dendrocronología, Instituto de Silvicultura, Universidad Austral de Chile, Valdivia, Chile.

³Now at Department of Earth and Atmospheric Science, State University of New York at Albany, Albany, New York, USA.

weather forecasting, climate prediction and the study of specific mesoscale circulation systems in South America [e.g., *Roads et al.*, 2003; *Seth and Rojas*, 2003; *Rojas and Seth*, 2003; *Seth et al.*, 2004, 2007; *Fernandez et al.*, 2006; *Rauscher et al.*, 2006, 2007; *Rojas*, 2006] but with a few exceptions [*Fuenzalida et al.*, 2007; *Garreaud and Falvey*, 2008; *Cook and Vizu*, 2008] they have not focused on future climate change scenarios and to our knowledge, none so far have focused specifically on the tropical Andes. This mountain region provides a particular challenge for climate modeling given the complex topography and the steep climatic gradients ranging from tropical rain forest on the eastern slopes to absolute desert along the Pacific coast. Since GCMs are not capable of adequately resolving these climatic gradients, some studies have tried to circumvent this problem by instead analyzing projected temperature changes in the free troposphere [*Bradley et al.*, 2004, 2006], but this is not a suitable approach for surface variables such as precipitation. Regional climate models could yield the most significant improvement as they are better suited to resolve the geographic complexity of regional climate. Here we use the Hadley Centre Regional Climate Modeling System, PRECIS (Providing REgional Climate for Impact Studies), nested in the Hadley Centre Atmospheric Model version 3 (HadAM3) to assess how climate changes under two different IPCC-SRES scenarios, A2 and B2 between 1961 and 1990 and 2071–2100. We limit our discussion to variables known to affect glacier energy and mass balance, such as temperature and precipitation [e.g., *Franco et al.*, 2003, 2004; *Vuille et al.*, 2008b]. Our model domain includes entire tropical South America, but we will focus primarily on changes in the Andes as we are particularly interested in seeing whether certain changes in climate are elevation-dependent and whether this elevation dependence (e.g., temperature lapse rate) is a robust feature of the climate system or will change under varying greenhouse gas scenarios. Several analyses are performed separately for the eastern and western Andean slopes, as observational studies indicate significant differences in current climate trends [*Vuille and Bradley*, 2000]. A more detailed assessment of changes in variables other than temperature and precipitation, including the atmospheric circulation and of changes in the lowlands to the east of the Andes will be provided elsewhere.

[3] The next section provides a description of the RCM and other data sets used in this study. Section 3 presents an assessment of how realistically the model simulates current climate as well as a detailed analysis of how temperature and precipitation will change under future emission scenarios. We end with a critical discussion of our results and their implications in section 4, which also includes recommendations for future research on this topic.

2. Data and Methods

[4] The model domain corresponds to South America between approximately 10°N–27°S and 86°W–44°W (Figure 1), but in our analysis we focused mainly on the Andes region to detect and assess climatic changes at high elevations.

[5] We use the Hadley Centre Regional Climate Modeling System, PRECIS, with a 0.44° latitude × 0.44° longi-

tude (~50 × 50 km) resolution, to assess changes in climate between today and the end of the 21st century. PRECIS is based on the third generation Hadley Centre Regional Climate Model (HadRM3), nested in the Hadley Centre Atmospheric Model version 3 (HadAM3). The regional model includes 19 vertical levels from the surface to approximately 30 km in the stratosphere and solves a hydrostatic version of the full primitive equations on a spherical-polar grid [*Jones et al.*, 2004]. PRECIS has been successfully applied in previous studies to assess future changes in precipitation and cloud formation in Costa Rica [*Karmalkar et al.*, 2008], changes in coastal wind strength off the west coast of South America [*Garreaud and Falvey*, 2008], extreme events in China [*Zhang et al.*, 2006] and climate in Bangladesh [*Nazrul Islam et al.*, 2008].

[6] We performed three different simulations to analyze future climate change in the tropical Andes. The first simulation (RCM-20C) is a 30-year (1961–1990) control run, which provides the baseline for comparison with scenarios that include increased 21st century greenhouse gas concentrations. The lateral boundary conditions are provided by HadAM3, the global driving model, which has an improved physical parameterization [*Pope et al.*, 2001] and a relatively high horizontal resolution (1.25° latitude × 1.87° longitude). Sea surface temperature (SST) and sea-ice extent are prescribed from observations (HadISST1) [*Rayner et al.*, 2003].

[7] Two 21st century simulations with increased greenhouse gas concentrations (scenarios RCM-A2 and RCM-B2) were equally laterally forced with HadAM3, but based on results from IPCC-SRES scenarios A2 and B2. Changes in future SST were derived by adding the estimated changes and a linear trend during 2071–2100 from the corresponding run (HadCM3) to the observed HadISST values [*Jones et al.*, 2004]. The interannual SST variability between control and SRES runs therefore remains the same. RCM-A2 is based on a medium-high emission and high population-growth scenario (15 billion people and 850 ppm of CO₂ concentration by 2100) for the 2071–2100 period [*Giorgi and Bi*, 2005]. RCM-B2 on the other hand, corresponds to a lower-emission scenario with reduced population growth (10.4 billion people and 550 ppm by 2100).

[8] Here we only report on model results for temperature and precipitation, which are considered to be of highest relevance to society, ecosystem integrity and glacier mass balance in the tropical Andes. The model performance was assessed by comparing results from RCM-20C with observational data for the same period. We extracted gridded monthly precipitation and temperature data over the RCM domain from the CRU TS 2.1. data set [*Mitchell and Jones*, 2005], available for the entire period 1961–1990 on a 0.5 latitude × 0.5 longitude grid. Since the CRU data are only available over land it was merged with 2.5 longitude × 2.5 latitude monthly Climate Prediction Center (CPC) Merged Analysis of Precipitation (CMAP) [*Xie and Arkin*, 1997] data to get an estimate for the model performance over nearby oceanic areas as well. However, unlike CRU, CMAP data are only available since 1979, as it represents a blend of observational in situ rain gauge measurements with satellite data. Model results from PRECIS were resampled onto the CRU grid for validation purposes. Where only model simulations are compared (e.g., difference between 2071

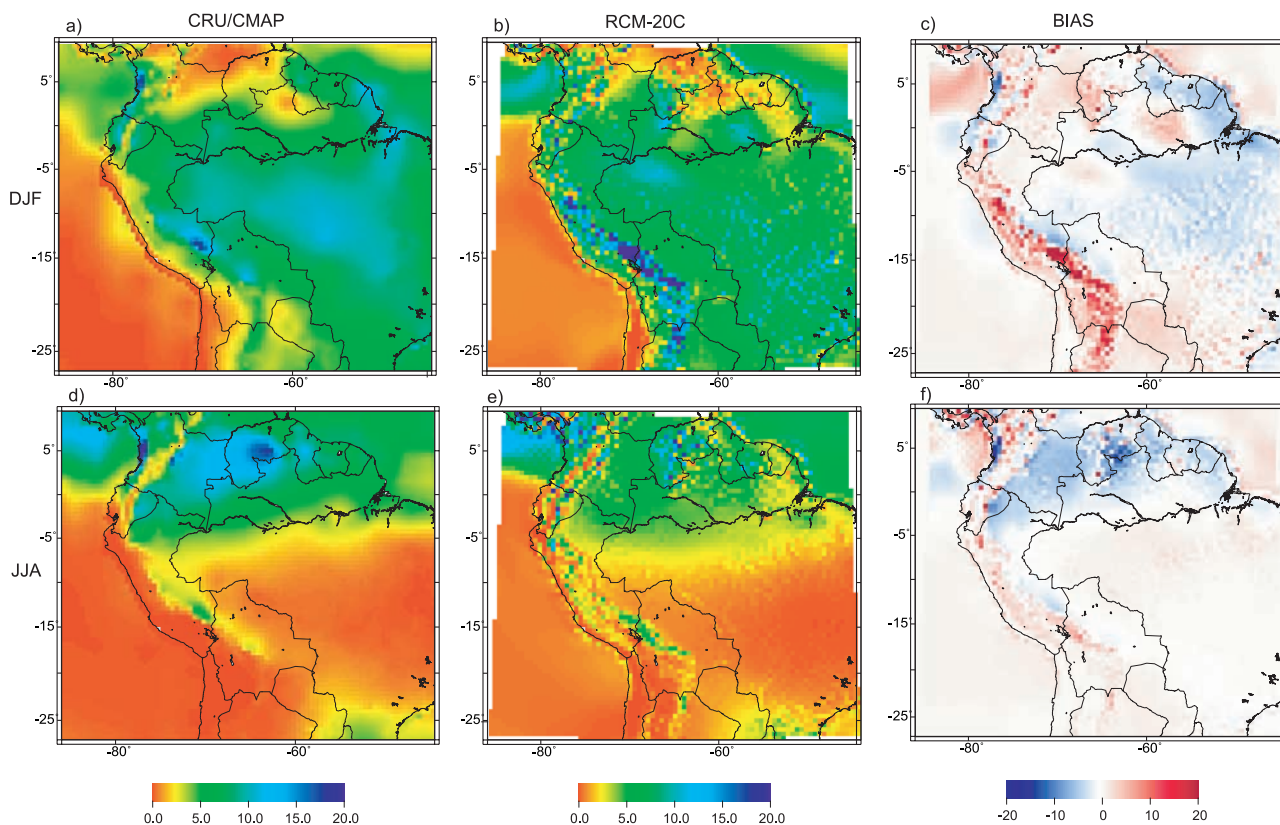


Figure 1. (a) Observed DJF precipitation (mm d^{-1}) based on CRU (land, 1961–1990) and CMAP (ocean, 1979–1990). (b) Same as in Figure 1a but for simulated precipitation (1961–1990) in RCM-20C. (c) Difference between CRU/CMAP and RCM-20C. (d, e, and f) Same as in Figures 1a–1c but for JJA.

and 2100 and 1961–1990) the original model grid was retained. Since temperature is highly dependent on the underlying grid topography, we also included observational in situ data from stations in the Andes. All station data were quality-controlled on the basis of difference time series with homogenized reference stations [Vuille and Bradley, 2000; Vuille et al., 2003].

[9] Projections of future climate change are assessed by analyzing both differences in the mean state of temperature and precipitation (annual and seasonal means) between RCM-20C and both RCM-A2 and RCM-B2, as well as changes in their statistical distribution (probability density functions, PDFs). The analysis of PDFs was performed to assess changes in the width or amplitude of the distribution between different scenarios. It was also used to assess whether present conditions and future scenarios overlap in their statistical distributions (e.g., if the warmest years in a control run could provide a modern analog for the coldest years in a future RCM-A2 or RCM-B2 scenario) and whether there might be an increased likelihood for extreme outliers in future climate scenarios (e.g., if the variability is much larger in a future greenhouse climate than it is today).

[10] We also include estimates of elevation-dependent changes in temperature and precipitation between 100 and 5000 m.a.s.l., separately for the eastern and western slope. To perform this analysis, the highest grid cell was chosen at each latitude along a N-S transect throughout the Andes

Cordillera, effectively dividing the Andes into an eastern and a western side. The eastern and western slopes include all grid cells to the east and west of the highest grid cell, respectively, as long as they are located within ~ 500 km (10 grid cells) of the Andean divide and >100 m a.s.l. Along the eastern slope the minimum threshold was set to an altitude of 400 m to exclude lowland grids located too far away from the Andes.

[11] Besides identifying changing conditions at the surface, we also analyzed projected temperature changes in the free troposphere for both RCM-A2 and RCM-B2 scenarios. In each case tropospheric temperature changes along latitudinal transects following the Andean crest were plotted. To draw the panels in Figure 10 in section 3.5, only the highest grid points along this transect and their immediate neighbors to the east and to the west were considered. The average value from these three grid cells was used to plot the free-tropospheric temperature above that altitude. As temperature is related to pressure rather than altitude in the model, a polynomial function using geopotential height was used to obtain the temperature at different elevation levels.

[12] Whenever modern conditions and future scenarios were compared a two-tailed Student's t test considering unequal variances and 95% confidence levels was performed to determine if mean values (annual or seasonal) were significantly different between the two scenarios.

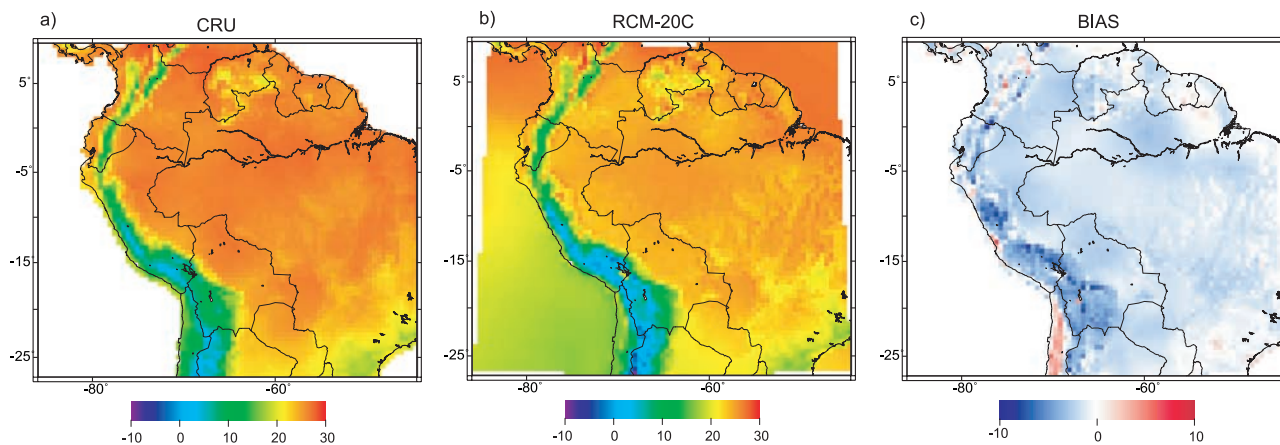


Figure 2. (a) Observed annual mean surface air temperature (SAT) in °C based on CRU (1961–1990). (b) Same as in Figure 2a but for RCM-20C. (c) Difference between CRU and RCM-20C.

Unless noted otherwise statistical significance always refers to the 95% significance level.

3. Results

3.1. Comparison of RCM-20C With Observations

[13] The seasonal distribution and spatial variations of precipitation are quite accurately simulated by the model (Figure 1), but the total amounts are slightly underestimated over eastern South America and significantly overestimated along the eastern slope of the Andes in DJF. This excess precipitation near the Andes is a common problem in many RCMs [e.g., *Roads et al.*, 2003; *Fernandez et al.*, 2006] and even in NCEP reanalysis data [e.g., *Costa and Foley*, 1998; *Liebmann et al.*, 1998]. During austral winter (JJA) precipitation amounts in the Andes are much closer to observations.

[14] The model also has a cold bias (Figure 2) exacerbated over higher terrain. The strong cooling over the Andes may be related to the excess precipitation, which reduces incoming solar radiation and lowers air temperature over the

eastern Andean slope. In some individual grid cells the temperature difference can amount to several degrees Celsius. A similar cold bias in the Andes was found in RegCM3 by *Fernandez et al.* [2006]. *Karmalkar et al.* [2008] also found a cool bias in the PRECIS model over Costa Rica, with temperature differences between model and CRU data also increasing over higher terrain. This comparison of temperature between model and CRU data, however, should be interpreted with caution, as the two data sets depend on the underlying topography which is different in the two data sets. Hence Figure 2 actually compares grid cells at the same location but with different elevation. We therefore also compare the CRU and RCM-20C data with observations from the Andes (station data) by plotting mean annual temperature versus elevation (Figure 3). The observations were extracted from an Andean climate database which includes 279 station records between the 1°N and 23°S [*Vuille and Bradley*, 2000]. Hence the observational record only covers the Andes south of the equator (mainly Ecuador, Peru, Bolivia and northernmost Chile), but does

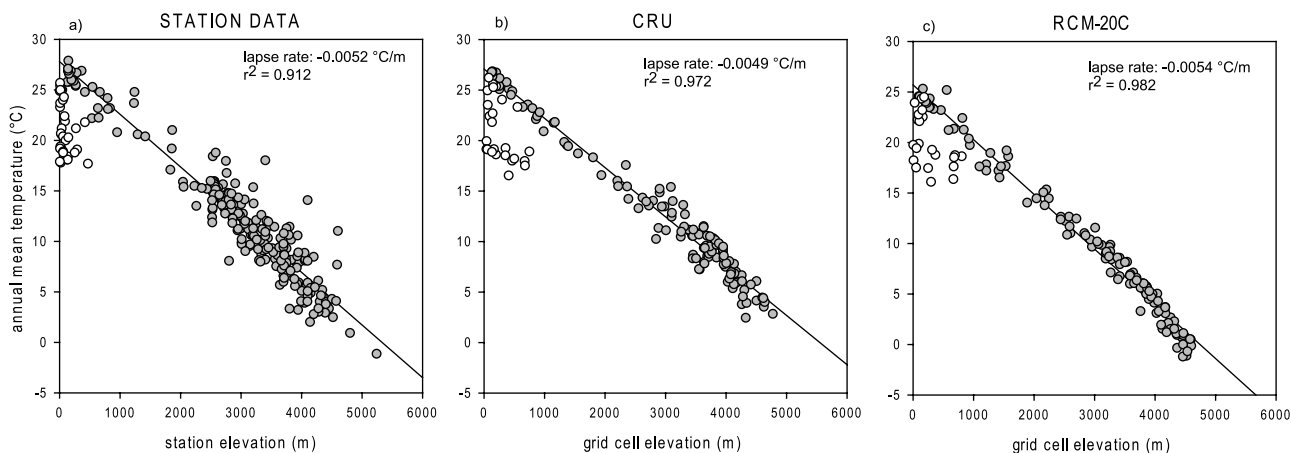


Figure 3. (a) Scatterplot of long-term mean (1961–1990) annual surface air temperature (in °C) versus elevation based on station data. Open circles (low-elevation stations on the western slope) were excluded from the lapse rate calculation. See text for details. (b) Same as in Figure 3a but for CRU data, subsampled to match location of station data in Figure 3a. (c) Same as in Figure 3a but for data from RCM-20C, subsampled to match location of station data in Figure 3a.

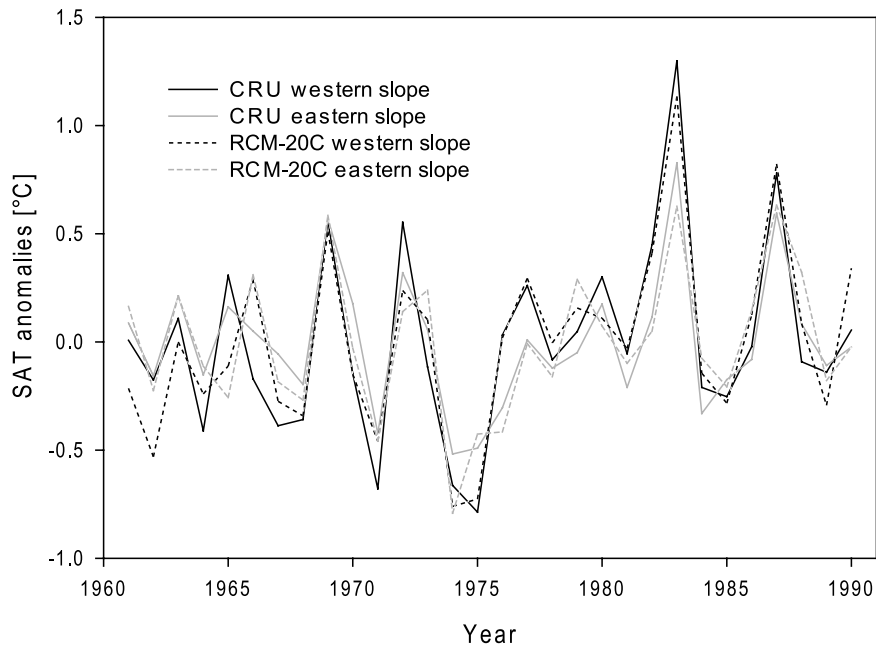


Figure 4. Time series of interannual variability in annual mean surface air temperature between 1961 and 1990 on the eastern and western slopes of the Andes based on observations (CRU) and model (RCM-20C).

not include data from Colombia and Venezuela. Individual records were gridded on to a 0.5 latitude \times 0.5 longitude grid by averaging all records located within each grid cell. Since many grid cells did not have any temperature data and were left blank, both CRU and RCM-20C data were subsampled to match the location of the station data. The results show that the model does indeed have a cold bias, especially at the highest elevations, but they also indicate that the CRU data is probably too warm over the Andes and that the true lapse rate lies somewhere in the middle between CRU and PRECIS. The open circles in Figure 3

are low-elevation stations to the west of the Andes, which are influenced by the cold Humboldt Current and therefore much colder than their counterparts to the east. These data points were excluded from the regression calculation. Figure 4 shows the interannual variability of annual mean surface temperature as simulated by RCM-20C and as recorded in the CRU data. Clearly the model is able to closely track interannual variations in temperature, which primarily reflect SSTA in the tropical Pacific [Vuille *et al.*, 2000a, 2000b] on both sides of the Andes. Correlation coefficients between the observed and simulated time series

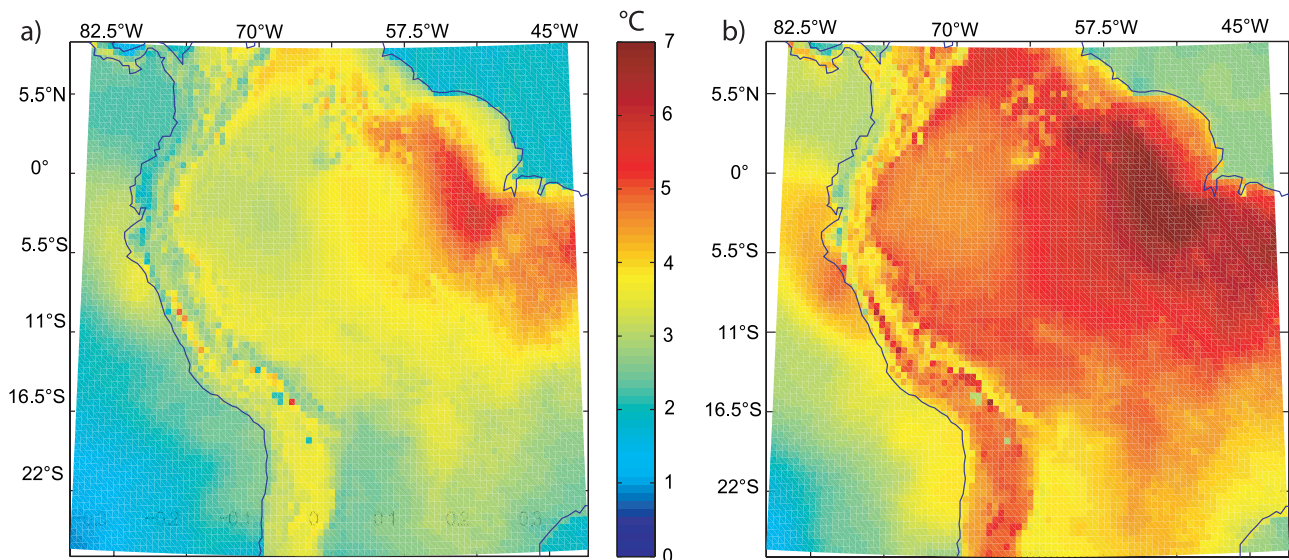


Figure 5. (a) Difference in mean annual surface temperature (in $^{\circ}\text{C}$) between RCM-B2 and RCM-20C. (b) Same as in Figure 5a but for RCM-A2. Differences are statistically significant at the 95% level everywhere.

displayed in Figure 4 are 0.90 for the western and 0.84 for the eastern slope, both significant at $p < 0.01$.

3.2. Changes in Surface Temperature and Precipitation

[15] Keeping these model shortcomings in mind, we next compare results from the control run, RCM-20C with the 21st century scenarios RCM-A2 and RCM-B2. Figure 5 shows the difference in simulated mean annual surface air temperature between RCM-A2 and RCM-B2 when compared with the control run, RCM-20C. The spatial pattern is almost the same in both simulations, but the magnitude varies considerably. In some areas the warming is up to 3°C larger in RCM-A2 than in the RCM-B2 scenario. Extreme warming is also more widespread in RCM-A2 than in RCM-B2, in particular in northeastern South America. Along the Andes, projected changes in temperature are also up to 3°C larger in RCM-A2, when compared to the RCM-B2 scenario. The largest high-elevation warming is projected for the Cordillera Blanca in Peru ($\sim 8.5^{\circ}\text{S}$ – 10°S), the most extensively glaciated tropical mountain range in the world. A t test reveals that temperature differences between the future scenarios (RCM-A2 and RCM-B2) and RCM-20C are all significant throughout the entire domain. Our results are consistent with previous analyses of predicted temperature changes based on GCMs, which also show that different scenarios produce the same pattern of warming and that the main difference between scenarios lies in their amplitude rather than in their spatial expression of projected changes [Boulangier *et al.*, 2006].

[16] There is a close coupling between the Equilibrium Line Altitude (ELA) and the 0°C isotherm in the inner tropics [Greene *et al.*, 2002]. It is therefore of interest to see how large of an area might be affected by a future rise of this freezing line. In our simulations, areas with an annual mean temperature below freezing decrease by 95% and 85%, in the RCM-A2 and RCM-B2 scenarios, respectively. During the austral summer months temperature even rises above 0°C everywhere in the RCM-A2 scenario. However, it should be kept in mind that the RCM grid resolution does not sufficiently resolve the highest peaks in this region of complex topography and that this estimate is therefore an underestimation of the true area that resides above the freezing line.

[17] Absolute and relative changes in precipitation between the RCM-A2 and control scenarios for annual and seasonal periods are shown in Figure 6. Given that the spatial pattern of precipitation change is similar for all emission scenarios [Boulangier *et al.*, 2007], but that RCM-A2 shows the strongest response, we limit our discussion to this scenario. Owing to the significant seasonality of precipitation in the tropics we show results separately for austral summer, December–February (DJF), and winter, June–August (JJA). The largest increase in annual precipitation (up to 2000 mm) occurs in the northern tropical Pacific off the coast of Panama and Colombia, and in the

coastal areas of the latter. An increase of similar magnitude is observed in the coastal region of Ecuador and in some places along the eastern Andes south of the equator. The largest relative increase occurs over the Pacific Ocean and along the coast of Ecuador and northern Peru (between 0° and 8°S approximately), but also along the coastline farther to the south. The largest decrease both in absolute and relative terms takes place in northeastern South America and the adjacent Atlantic Ocean (a decrease of up to 1600 mm and more than 50%). Changes in the Andes and their significance are not spatially coherent and include both regions of increased and decreased precipitation.

[18] The difference in austral summer precipitation is very similar to the annual difference, which is not surprising since these months represent the major wet season for most of tropical South America south of the equator. The largest absolute and relative increase in austral summer precipitation also takes place over the ocean and coastal area of Ecuador and northern Peru (between approximately 0° and 8°S – 9°S) and farther south along the west coast of South America. The largest relative reduction in precipitation (up to 80%) is projected for north-northeastern South America, including parts of Venezuela and Colombia, and coincides with the region of largest warming (see Figure 5). The increase in precipitation south of $\sim 0^{\circ}\text{S}$ suggests an enhanced monsoon by the end of the century. Differences in JJA precipitation reflect a more uniform pattern of reduction in precipitation throughout much of South America, with an increase over the western and a decrease over the eastern Amazon basin. A large and significant increase of more than 500 mm is simulated over the Pacific Ocean off the coast of Ecuador, Colombia and Panama. The largest relative increase in austral winter precipitation is displayed along the coast south of 0°S , and over the ocean north of 0° , while the largest decrease occurs in the eastern part of the study area, and also in some areas of the Andes south of 20°S (up to 100%).

3.3. Changes in Surface Temperature and Precipitation Versus Elevation Along the Andes

[19] Figure 7 shows the decrease of mean annual surface temperature with altitude separately for the western and eastern slope in both RCM-20C and RCM-A2. As above, we limit our discussion to the results of the RCM-A2 scenario. The difference plots are helpful to highlight the elevation zones which are projected to warm the most and the least. On the western side of the Andes a rather abrupt change in the temperature lapse rate occurs near 2500 m a.s.l. (Figure 7a), with an extremely low lapse rate of only -0.38°C per 100 m at low elevations. This break is equally apparent in the RCM-A2 simulation (Table 1). The low lapse rate is likely a reflection of the low-level subsidence region over the SE Pacific, maintained by the cold Humboldt Current and its associated upwelling effect which tends to cool the overlying atmosphere and the lower

Figure 6. Absolute difference in (a) mean annual, (b) DJF, and (c) JJA precipitation totals (in millimeters) between RCM-A2 and RCM-20C. Note different scale in Figures 6b and 6c. (d, e, and f) Same as in Figures 6a–6c but for relative difference (in percent). (g, h, and i) Dark (light) brown areas indicate regions where the difference is statistically (not) significant at the 95% level. Figure 6g refers to Figures 6a and 6d, Figure 6h refers to Figures 6b and 6e, and Figure 6i refers to Figures 6c and 6f.

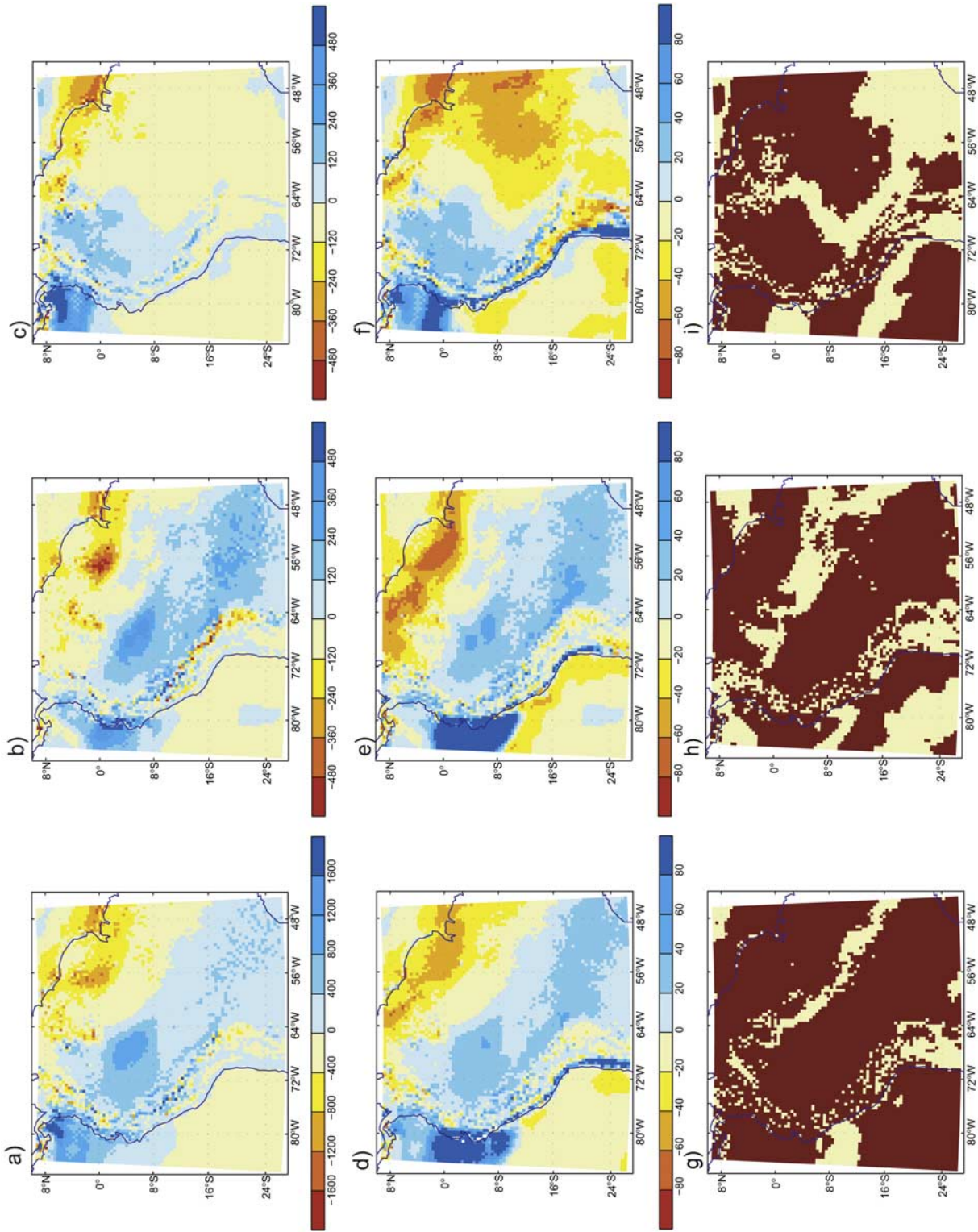


Figure 6

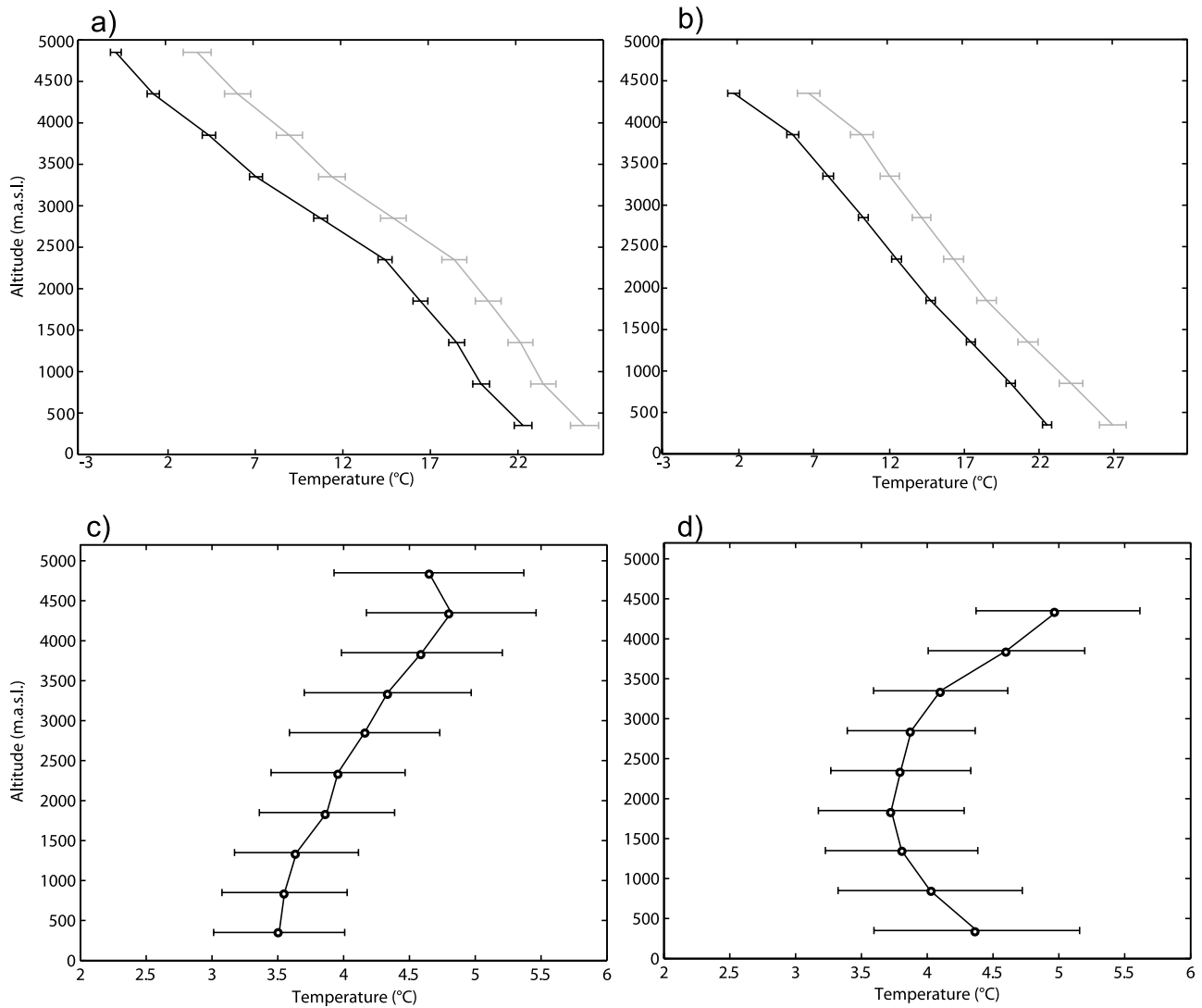


Figure 7. (a) Mean annual surface air temperature at different altitude levels for RCM-20C (black) and RCM-A2 (gray) along the western slope of the Andes. Horizontal bars correspond to the standard deviation of mean annual air temperature at different altitude levels. (b) Same as in Figure 7a but along the eastern slope of the Andes. Note different scale. (c) Difference in temperature between RCM-A2 and RCM-20C for the western slope of the Andes. Horizontal bars correspond to the standard deviation of the difference in temperature at different altitude levels. Black circles indicate that annual mean temperature values between both scenarios are significantly different at the 95% level. (d) Same as in Figure 7c but for the eastern slope of the Andes.

Andean slopes (see also Figure 3). Hence temperatures are warmer on the eastern than on the western slope at lower altitudes (below 1000 m) in the RCM-20C and RCM-A2 scenario. Between 1000 and 3000 m, temperature is higher on the western slope, but above this altitude temperature is again higher on the eastern slope. As expected, there is a general trend to lower lapse rate values in the RCM-A2 scenario except for the lower level on the eastern slope. Especially noticeable is the significant decrease in lapse rate at higher altitudes along the eastern slope of the Andes (Table 1). Note that the lapse rates are calculated over the entire Andean domain and therefore are not comparable with the values calculated in Figure 3, which were subsampled to match the location of the available station data. As mentioned above, temperatures at the highest elevation

pass from below freezing in RCM-20C to well above freezing along the western slope in the RCM-A2 scenario. Given the lack of vertical resolution in our RCM the exact implications of this rise in freezing levels for Andean glaciers remains unclear. It is obvious however, that the higher temperatures will lead to a significant rise in the rain-snowline, and the increased exposure of glaciers to rain as opposed to snow is known to have negative impacts for tropical glacier mass balance, even on interannual time-scales [Francou *et al.*, 2004]. Standard deviations are higher in all cases for the RCM-A2 scenario on both slopes. Figure 7c shows that there is an increase in projected warming with elevation on the western slope ranging from 3.5°C at 500 m to approximately 4.8°C above 4000 m a.s.l., significant at all altitude levels. Along the eastern slope

Table 1. Lapse Rates for the Western and Eastern Slope of the Andes in the RCM-20C and RCM-A2 Scenarios and for Three Altitude Ranges^a

Altitude Ranges (m)	Lapse Rates Western Slope (°C/100 m)		Lapse Rates Eastern Slope (°C/100 m)	
	RCM-20C	RCM-A2	RCM-20C	RCM-A2
100/400–2500	-0.38	-0.36	-0.51	-0.54
2500–5000	-0.58	-0.56	-0.57	-0.49
100/400–5000	-0.54	-0.51	-0.50	-0.49

^aValues below 100 m and 400 m for the western and the eastern slope, respectively, were ignored.

(Figure 7d) there is also an increased warming signal at highest elevations (more than 4.5°C above 3500 m a.s.l.). In addition, there is also a large warming (approximately 4.4°C) projected at the lowest level (below 500 m a.s.l.). Again temperature changes are significant at all elevations.

[20] These projected changes do not entirely agree with the general pattern of warming found for observations between 1°N and 23°S by *Vuille and Bradley* [2000] and *Vuille et al.* [2003]. The observed 20th century warming is larger in the western than in the eastern Cordillera at lower elevations, especially below 1000 m. Between 2000 m and 3500 m observations and projections both suggest stronger warming over the western slope. At higher elevations, however, *Vuille and Bradley* [2000] and *Vuille et al.* [2003] observed a decrease in warming with elevation, while in this study warming is more pronounced at higher altitudes on both slopes of the Andes. This discrepancy between observed and projected warming may have various reasons. For one, observed temperature trends in the 20th century are not solely due to increasing greenhouse gas concentrations but also reflect natural climate variability. In addition the domain of the present study is enlarged and also includes regions to the north of 1°N, which was not sampled in

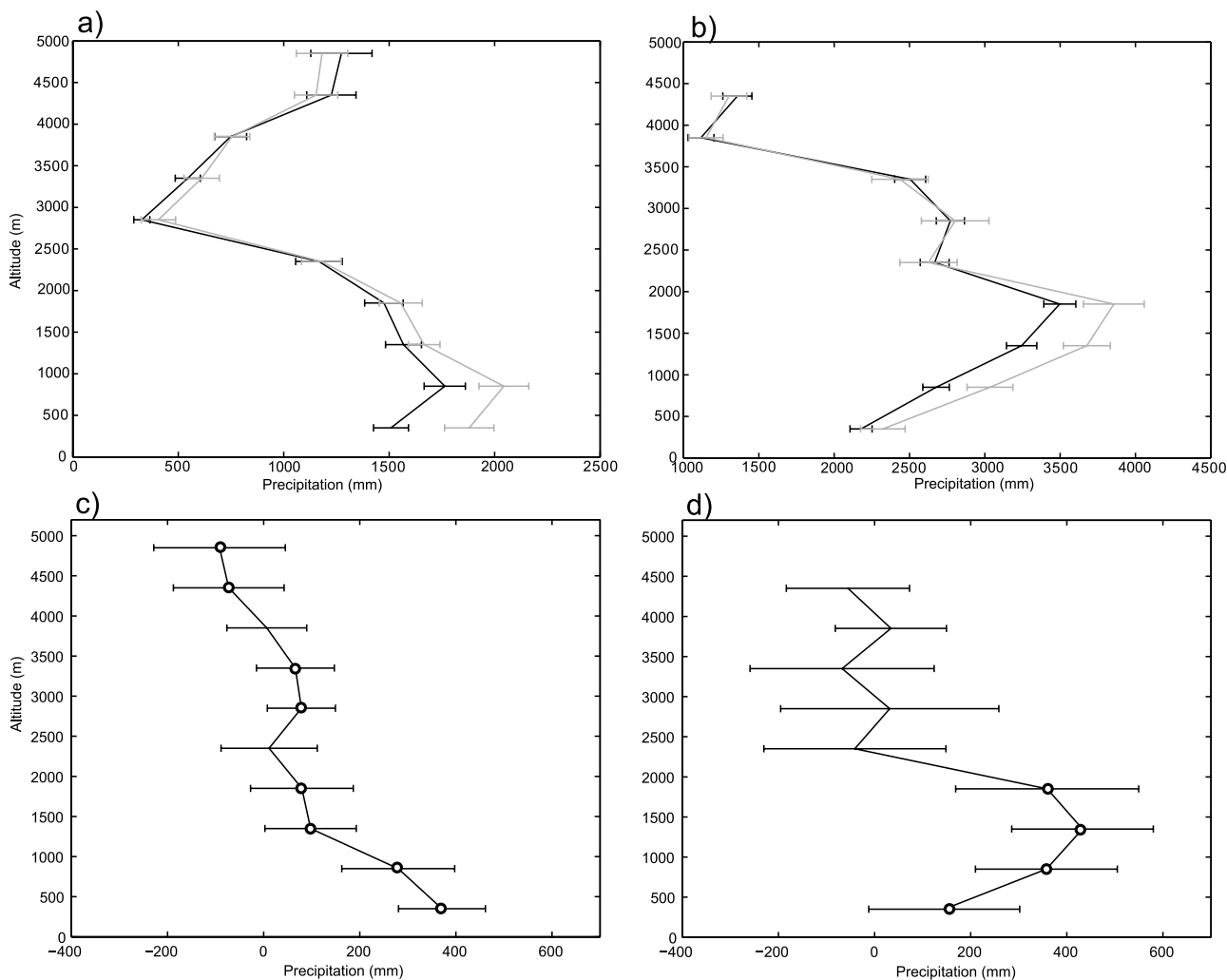


Figure 8. (a) Precipitation at different altitude levels for RCM-20C (black) and RCM-A2 (gray) along the western slope of the Andes. Horizontal bars correspond to the standard deviation of mean annual precipitation at different altitude levels. (b) Same as in Figure 8a but for the eastern slope of the Andes. Note different scale. (c) Difference in precipitation between RCM-A2 and RCM-20C for the western slope. Horizontal bars correspond to the standard deviation of the difference in precipitation at different altitude levels. Black circles indicate that annual mean precipitation values between both scenarios are significantly different at the 95% level. (d) Same as in Figure 8c but for the eastern slope of the Andes.

the mentioned observational studies. In any case our simulations suggest that the observed warming trend in the Andes and its elevation dependence may be altered in the future as a result of increased greenhouse gas concentrations.

[21] Figure 8 shows the variation of mean annual surface precipitation at different altitude levels for the western and eastern slope in RCM-20C and RCM-A2, as well as their difference. In both simulations precipitation increases along the western slope up to 1000 m a.s.l and decreases thereafter until approximately 3000 m a.s.l (Figure 8a). Above that point precipitation increases, but does not reach values as high as at lower elevation. However, it is important to keep in mind that this analysis averages precipitation over very a large latitudinal area with an extreme precipitation gradient, ranging from superhumid (Colombian coast) to extremely arid (Atacama Desert). Hence these absolute values and their vertical distribution should be interpreted with caution. For example the major increase in precipitation along the western slope at lower elevations is by and large a reflection of the large increase in precipitation projected for coastal areas of Ecuador and northern Peru (Figure 6). In general the projected changes in precipitation are not as pronounced as for temperature. Largest absolute changes are present at the lowest altitude level. In general, precipitation is slightly higher in the RCM-A2 scenario below 4000 m a.s.l. and slightly less beyond that elevation (Figure 8a).

[22] Along the eastern slope precipitation increases with altitude up to 2000 m a.s.l, above which point it mostly decreases (Figure 8b). Significant increases are projected for areas below 2500 m a.s.l. in the RCM-A2 scenario. Above this altitude differences are small and insignificant (Figure 8d). In general standard deviations are higher for the RCM-A2 scenario on both slopes.

[23] In summary a general increase in precipitation might be expected, at least up to 2000 m a.s.l., for both slopes of the Andes. Above that altitude no significant changes (eastern slope) or even a decrease in precipitation (western slope, above 4000 m) is projected by our simulations. This would suggest that a more negative glacier mass balance, caused by larger warming at higher altitudes, may not be offset by increased precipitation.

3.4. Probability Density Functions for Surface Temperature Along the Andes

[24] Figure 9 shows the PDFs for RCM-20C, RCM-A2 and RCM-B2 scenarios for both western and eastern slopes. Vertical bars indicate the actual years in each distribution. The mean annual temperature along the western slope increases from 15.35°C (RCM-20C), to 18.25°C (RCM-B2) and 19.25°C (RCM-A2), respectively (Figure 9a), indicating a shift in the mean annual temperature of 2.9°C (RCM-B2) and 3.9°C (RCM-A2). The standard deviation also increases by 78% from 0.41°C (RCM-20C) to 0.73°C (RCM-A2), but remains almost unchanged (0.43°C) in RCM-B2 (Table 2).

[25] Temperature along the eastern slope of the Andes is roughly 3°C colder than on the western side (Figure 9b). However, since the lower-elevation threshold of grid cells included in this study is 400 m on the eastern side, but 100 m on the western side, these values are not directly comparable. The temperature increase on the eastern slope corresponds to 3.1°C (4.2°C) in RCM-B2 (RCM-A2), slightly

more than the increase projected for the western slope. The change in the standard deviation is also much larger, corresponding to approximately 118% in RCM-A2. This larger increase reflects the much lower standard deviation on the eastern slope in the control run when compared to the west. Indeed the RCM-A2 standard deviations only differ by 0.01°C between both slopes (Table 2). Changes in mean temperature are significant in all cases (both slopes and both scenarios), but changes in standard deviation are only significant in the RCM-A2 scenario (both slopes). In addition, it is noteworthy that on both slopes the temperature of the warmest year in the control run is well below the temperature of the coldest year in future predictions, even for the lower-emission B2 scenario. This suggests a complete lack of a modern analog in the observational record and is indicative of the drastic change in the overall mean conditions in the future. The most obvious difference between RCM-A2 and RCM-B2 scenarios on both slopes appears to be the less pronounced change in standard deviation in the RCM-B2 run. This suggests that a future RCM-B2 climate might be warmer, but with an interannual variability similar to today, very much unlike what is projected for the RCM-A2 scenario.

3.5. Changes in Free Tropospheric Temperature

[26] Figure 10 shows the difference in annual, DJF and JJA mean free-tropospheric temperature between RCM-A2, RCM-B2 and the control scenarios, RCM-20C. Temperature trends were assessed on ten different pressure levels (1000, 925, 850, 700, 600, 500, 400, 300, 250 and 200 hPa) and then converted to elevations a.s.l. using geopotential height. In all scenarios and seasons projected warming increases with altitude and decreases with increasing latitude, consistent with previous studies [Bradley *et al.*, 2004, 2006]. The warming rate varies between 2.5°C (3.5°C) at approximately 2000 m and 5.5°C (7.5°C) at approximately 12,000 m in RCM-B2 (RCM-A2). The larger difference between low- and high-altitude temperature change in the RCM-A2 scenario implies a larger reduction in the free-tropospheric lapse rate. The tropospheric warming shows some seasonal bias with slightly (~1°C) stronger warming in JJA than in DJF. This suggests a smaller future amplitude of the seasonal cycle especially in the outer tropics, a condition also observed for surface temperature (not shown). In all cases (annual, DJF and JJA), changes are significant for both the RCM-A2 and RCM-B2 scenarios.

4. Discussion and Conclusions

[27] Our simulations with a nested RCM suggest significant changes in tropical Andean climate toward the end of the 21st century. The model displays a cold and wet bias in its mean state, in particular along the eastern Andean slopes, but the seasonal cycle and interannual variability are simulated fairly accurately. Climate in tropical South America at the end of the 21st century is dominated by a significant warming over the entire model domain, with temperature increasing between 2° and 7°C depending on location and scenario considered. In general, enhanced warming is projected for JJA (not shown), suggesting a smaller amplitude of the seasonal cycle. Differences between the RCM-A2 and RCM-B2 scenarios are mainly in magnitude (up to 3°C

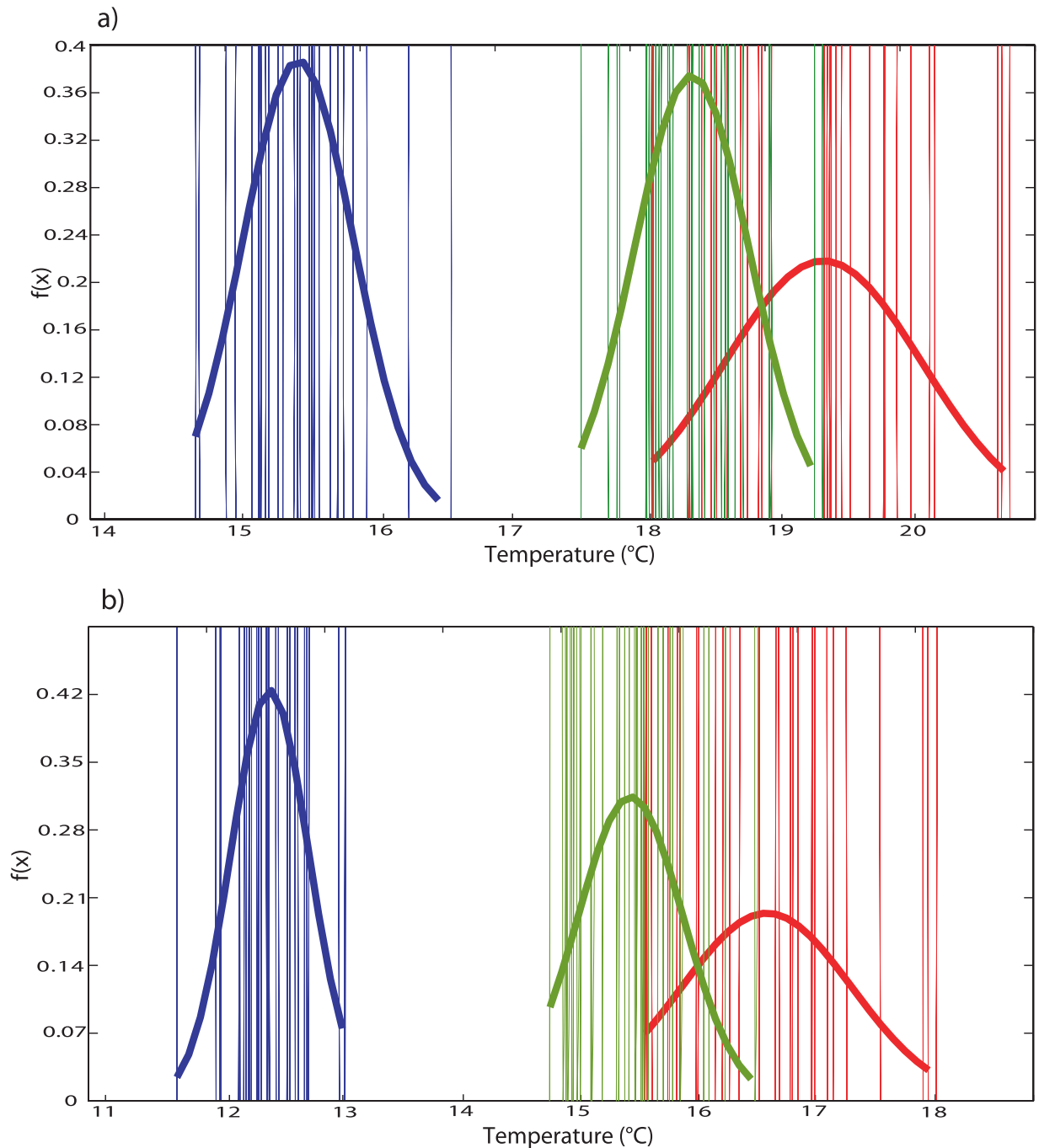


Figure 9. (a) PDFs for mean annual temperature for RCM-20C (blue), RCM-B2 (green), and RCM-A2 (red), along the western slope of the Andes (>100 m). Thin vertical lines represent the individual years for each simulation. (b) Same as in Figure 9a but for the eastern slope of the Andes (>400 m).

warmer in the A2 scenario), while the spatial pattern of warming is essentially unchanged, consistent with previous studies [Boulangier *et al.*, 2006]. Inspection of the temperature PDF on both slopes of the Andes further reveals that there is no overlap between mean annual temperatures of the control run (RCM-20C) and either of the two future scenarios (RCM-A2 and RCM-B2). Clearly the warmest temperature in the control run are much lower than the coldest temperatures projected for the years 2071–2100. In addition

significant changes in variability (a wider distribution) are expected for the RCM-A2 scenario but not for RCM-B2.

[28] In the free troposphere the largest warming is expected to occur in the upper troposphere during JJA, thereby decreasing the seasonal amplitude in the outer tropics (as in the case of surface temperature). The projected changes are very similar to the results obtained by averaging eight different GCMs used in the IPCC AR4, also based on the A2 scenario [Bradley *et al.*, 2006]. In both projections

Table 2. Average Temperature and Standard Deviation in Each PDF for Each Scenario and Slope of the Andes^a

	RCM-20C		RCM-A2		RCM-B2	
	μ	σ	μ	σ	μ	σ
Western slope	15.35	0.41	19.25	0.73	18.25	0.43
Eastern slope	12.35	0.33	16.55	0.72	15.45	0.44

^aAverage temperature, μ ; standard deviation, σ . Temperature and standard deviation given in °C.

the rate of warming increases with altitude, but the largest temperature change ($>7^{\circ}\text{C}$ in both studies) is reached at a lower altitude in the projection using the GCMs. This may to some extent be an artifact of the different time periods used to calculate the tropospheric warming trend (*Bradley et*

al. [2006] used the time period 2090–2099 minus 1990–1999) or the differences in both vertical and horizontal resolution between GCMs and our RCM. However, looking at the temperature change surrounding the highest mountain peaks in the area depicted by *Bradley et al.* [2006] and in an update provided by *Vuille et al.* [2008a], temperature changes are quite similar and at most 0.5°C higher in the GCM-based study. More importantly, the midtropospheric warming in our study is internally consistent with the simulated high-elevation near-surface trends, confirming that midtropospheric temperature trends derived from GCMs may indeed be a suitable way to assess high-elevation climate change in mountain regions.

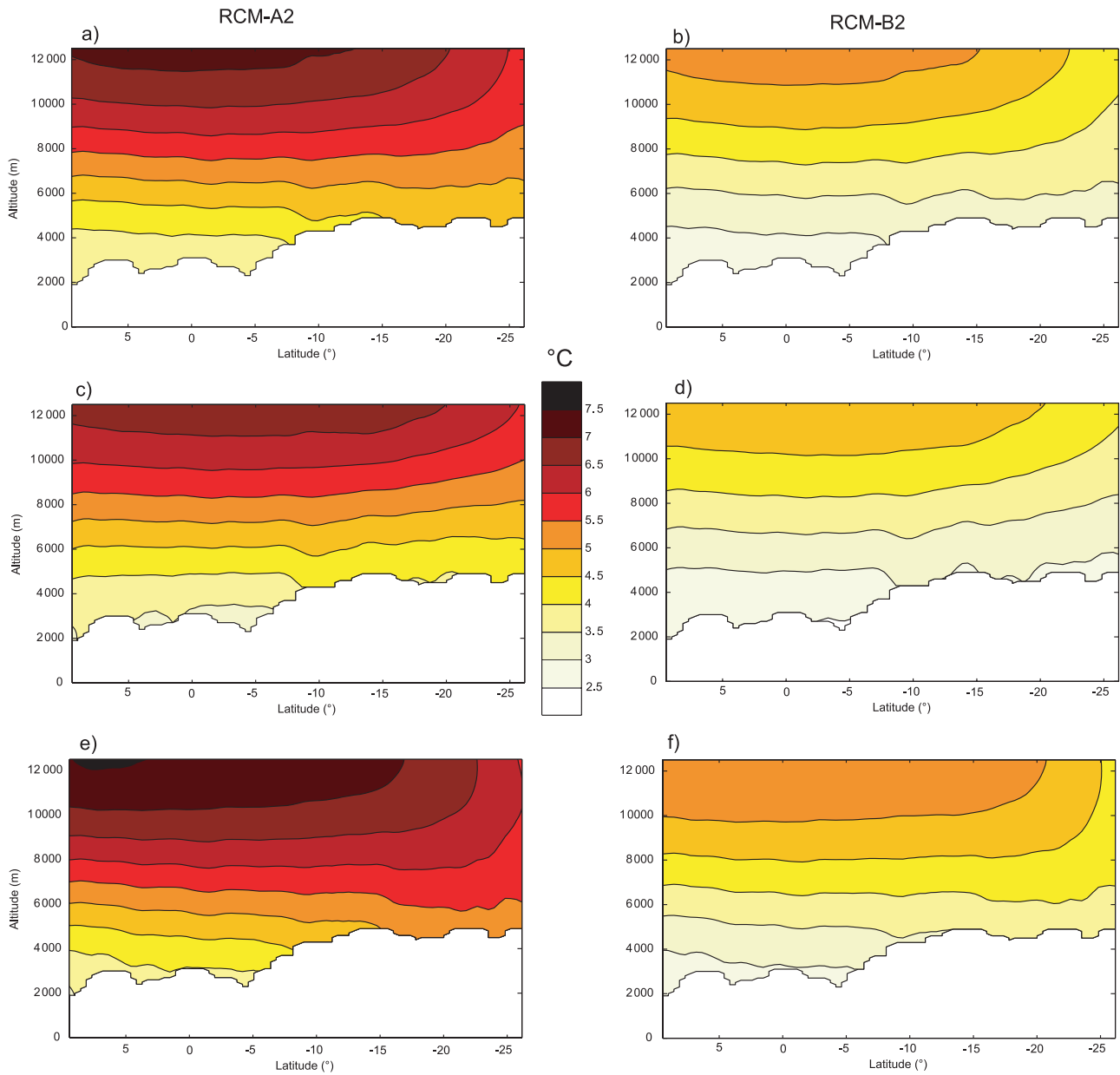


Figure 10. (a) Difference in annual mean free-tropospheric temperature between RCM-A2 and RCM-20C along a N-S transect following the Andean ridge. (b) Same as in Figure 10a but for RCM-B2. (c) Same as in Figure 10a but for DJF. (d) Same as in Figure 10c but for RCM-B2. (e) Same as in Figure 10a but for JJA. (f) Same as in Figure 10e but for RCM-B2.

[29] The projected precipitation changes at the end of the 21st century suggest enhanced monsoon (DJF) precipitation in southern tropical South America, and a general decrease in JJA precipitation, consistent with most IPCC AR4 models [Vera *et al.*, 2006; Christensen *et al.*, 2007]. Along the Pacific coast and the lower western slopes of the Andes enhanced precipitation might be related to a projected weaker and southward displaced SE Pacific subtropical anticyclone, which would allow more humid conditions to develop along the tropical west coast of South America [Urrutia, 2008; Christensen *et al.*, 2007]. At higher elevations in the Andes projected changes in precipitation present a mixed pattern with both regions of increase (mostly north of $\sim 12^{\circ}\text{S}$) and decrease (mostly south of $\sim 12^{\circ}\text{S}$). Precipitation amounts in the southern part of the tropical Andes are strongly modulated by the strength of the upper-level easterly flow during the wet season, which through downward mixing of easterly momentum over the Andean ridge, facilitates moisture influx from the lowlands to the east [Vuille, 1999; Garreaud, 1999; Garreaud *et al.*, 2003; Vuille and Keimig, 2004]. Analysis of the changes in the upper tropospheric zonal wind field across the tropical Andes shows a weakening of the wet season easterlies in the middle and upper troposphere (Urrutia [2008], not shown). The weakening of this upper-level easterly flow might explain why much of the Andes south of $\sim 12^{\circ}\text{S}$ do not show increased precipitation in RCM-A2, while the conditions in the adjacent lowlands to the east, where the upper tropospheric zonal flow is of less relevance, become more humid.

[30] It is interesting to note that the projected changes in precipitation over tropical South America in many ways resemble the pattern seen during the ENSO warm phase in South America. Since the interannual variability in SSTs is the same in all our simulations, the changes in precipitation are likely a reflection of a change in the mean state of the tropical Pacific, which in HadCM3 tends to show a more El Niño-like pattern [Li *et al.*, 2006]. There is however, little agreement between models about the impacts of increased greenhouse gas forcing on ENSO activity in the tropical Pacific [e.g., Cane, 2005; Collins and the CMIP Modelling Groups, 2005] and these results should therefore be interpreted with caution.

[31] In summary even the more optimistic RCM-B2 scenario projects significant changes in Andean climate by the end of the 21st century, which will likely lead to severe impacts on socioeconomic activity, Andean ecosystems and maintenance of their biodiversity. The tropical Andes also play a critical role for downstream water supply by retaining much of the precipitation falling at high elevation as ice in mountain glaciers or as water in tropical wetlands (páramos), before gradually releasing it over time [Kaser *et al.*, 2003; Buytaert *et al.*, 2006; Juen *et al.*, 2007]. Glaciers and wetlands therefore act as critical buffers against highly seasonal precipitation and provide water for domestic, agricultural or industrial use during the dry season, when rainfall is low or absent. This environmental service is often taken for granted, yet our projections indicate that it is being threatened by future climate change. A more detailed assessment of how climate change, as simulated in our study, would affect tropical glacier or wetland distribution

in the tropical Andes, is beyond the scope of this study. It is however, a question of utmost importance and will be addressed by correcting our RCM results for the observed wet and cold bias [e.g., Salzmann *et al.*, 2007] and linking it to impact models such as a tropical glacier-climate model [Juen *et al.*, 2007] and models of tropical Andean hydrology [Buytaert *et al.*, 2006].

[32] Finally it is important to keep in mind a few caveats which were not addressed in this study. Deforestation and land cover changes over the Amazon basin are of great importance for Andean climate as the Amazon basin is the major moisture source for Andean precipitation but also affects the large-scale atmospheric circulation through latent heat release [e.g., Lenters and Cook, 1997]. Land cover changes will also impact the carbon cycle, with uncertain feedbacks on climate [Cox *et al.*, 2004; Li *et al.*, 2006]. Such changes are hard to predict and were not included in our study. In addition, the complex interactions between regional and remote factors that contribute to the climate of South America [Garreaud *et al.*, 2008] make it difficult to account for all the changes that might occur in the future and could affect climate. An earth system model, capable of simulating changes in vegetation associated with climate and its feedbacks, changes in vegetation caused by human activity, and chemical processes, plus CO_2 feedbacks, is needed to provide the necessary information to address future changes with more confidence (especially owing to the large area covered by the Amazon forests). Moreover, it is vitally important to develop more and better predictions including regional climate models, so that changes at a more local scale can be assessed with a higher degree of certainty. In the case of the Andes our results demonstrate that the use of a higher-resolution model can significantly improve estimates of future climate. Additional and complementary analyses could also contribute to better understand probable future changes in climate along the Andes. These include the analysis of daily or pentad precipitation to analyze changes in extreme events such as droughts or floods or changes in the onset and demise of the monsoon system. Such an analysis would be key to better predict impacts of climate change on Andean glaciation as the delayed onset of precipitation (snowfall) and the associated prolonged exposure of dirty ice has been identified as one of the main culprits of enhanced ice wastage due to enhanced absorption of solar radiation through ice-albedo feedbacks [Francou *et al.*, 2003].

[33] This study constitutes a first attempt to simulate future climate change by means of a regional climate model for the tropical Andes and it is one of only a few assessing 21st century climatic conditions in tropical South America using an RCM [e.g., Cook and Vizu, 2008]. We are aware that our estimates are based on only one model with only one realization for each scenario. Clearly ensemble simulations using different perturbed initial states and comparisons across a range of RCMs will be needed to put our results into a more robust multimodel perspective. The largest uncertainty introduced into future estimates of regional climate change, however, is not related to internal model variability or intramodel differences, but instead result from unknown future trends in greenhouse gas emissions. By analyzing results from both high- and low-

emission scenarios we have tried to at least partially address this uncertainty.

[34] **Acknowledgments.** This study forms part of the M.Sc. thesis of R.U. at the University of Massachusetts, Amherst. R.U. was funded by a grant from the Fulbright Commission and with support from the University of Massachusetts, Amherst, and by IAI project CRN-2047. M.V. was funded by NSF-Project EAR-0519415. Many thanks to Ambarish Karmalkar for his assistance with Matlab. We are also grateful for the detailed comments by three anonymous reviewers, which helped us to considerably improve an earlier version of this manuscript.

References

- Boulanger, J. P., F. Martinez, and E. C. Segura (2006), Projection of future climate change conditions using IPCC simulations, neural networks and Bayesian statistics. Part 1: Temperature mean state and seasonal cycle in South America, *Clim. Dyn.*, *27*, 233–259, doi:10.1007/s00382-006-0134-8.
- Boulanger, J.-P., F. Martinez, and E. C. Segura (2007), Projection of future climate change conditions using IPCC simulations, neural networks and Bayesian statistics. Part 2: Precipitation mean state and seasonal cycle in South America, *Clim. Dyn.*, *28*, 255–271, doi:10.1007/s00382-006-0182-0.
- Bradley, R. S., F. Keimig, and H. Diaz (2004), Projected temperature changes along the American cordillera and the planned GCOS network, *Geophys. Res. Lett.*, *31*, L16210, doi:10.1029/2004GL020229.
- Bradley, R. S., M. Vuille, H. Diaz, and W. Vergara (2006), Threats to water supplies in the tropical Andes, *Science*, *312*(5781), 1755–1756, doi:10.1126/science.1128087.
- Buytaert, W., R. Celleri, B. De Bievre, F. Cisneros, G. Wyseure, J. Deckers, and R. Hofstede (2006), Human impact on the hydrology of the Andean páramos, *Earth Sci. Rev.*, *79*, 53–72, doi:10.1016/j.earscirev.2006.06.002.
- Cane, M. A. (2005), The evolution of El Niño, past and future, *Earth Planet. Sci. Lett.*, *230*, 227–240, doi:10.1016/j.epsl.2004.12.003.
- Ceballos, J. L., C. Euscategui, J. Ramirez, M. Canon, C. Huggel, W. Haeblerli, and H. Machguth (2006), Fast shrinkage of tropical glaciers in Colombia, *Ann. Glaciol.*, *43*, 194–201, doi:10.3189/172756406781812429.
- Christensen, J. H., et al. (2007), Regional Climate projections, in *Climate Change 2007: The Physical Science Basis. Contribution of Working Group I to the Fourth Assessment Report of the Intergovernmental Panel on Climate Change*, edited by S. Solomon et al., pp. 847–940, Cambridge Univ. Press, Cambridge, U.K.
- Collins, M. and the CMIP Modelling Groups (2005), El Niño- or La Niña-like climate change?, *Clim. Dyn.*, *24*, 89–104, doi:10.1007/s00382-004-0478-x.
- Cook, K., and E. Vizy (2008), Effects of twenty-first century climate change on the Amazon rain forest, *J. Clim.*, *21*, 542–560, doi:10.1175/2007JCLI1838.1.
- Costa, M. H., and J. A. Foley (1998), A comparison of precipitation datasets for the Amazon basin, *Geophys. Res. Lett.*, *25*, 155–158, doi:10.1029/97GL03502.
- Cox, P. M., R. A. Betts, M. Collins, P. P. Harris, C. Huntingford, and C. D. Jones (2004), Amazonian forest dieback under climate-carbon cycle projections for the 21st century, *Theor. Appl. Climatol.*, *78*, 137–156, doi:10.1007/s00704-004-0049-4.
- Fernandez, J. P. R., S. H. Franchito, and V. B. Rao (2006), Simulation of the summer circulation over South America by two regional climate models. Part I: Mean climatology, *Theor. Appl. Climatol.*, *86*, 247–260, doi:10.1007/s00704-005-0212-6.
- Francou, B., M. Vuille, P. Wagnon, J. Mendoza, and J. E. Sicart (2003), Tropical climate change recorded by a glacier in the central Andes during the last decades of the 20th century: Chacaltaya, Bolivia, 16°S, *J. Geophys. Res.*, *108*(D5), 4154, doi:10.1029/2002JD002959.
- Francou, B., M. Vuille, V. Favier, and B. Cáceres (2004), New evidence for an ENSO impact on low latitude glaciers: Antizana 15, Andes of Ecuador, 0°28'S, *J. Geophys. Res.*, *109*, D18106, doi:10.1029/2003JD004484.
- Fuenzalida, H., P. Aceituno, M. Falvey, R. Garreaud, M. Rojas, and R. Sanchez (2007), Study on climate variability for Chile during the 21st century (in Spanish), 63 pp., technical report, Natl. Environ. Comm., Santiago. (Available at <http://www.dgf.uchile.cl/PRECIS>)
- Garreaud, R. D. (1999), Multi-scale analysis of the summertime precipitation over the central Andes, *Mon. Weather Rev.*, *127*, 901–921, doi:10.1175/1520-0493(1999)127<0901:MAOTSP>2.0.CO;2.
- Garreaud, R. D., and M. Falvey (2008), The coastal winds of western subtropical South America in future climate scenarios, *Int. J. Climatol.*, in press.
- Garreaud, R., M. Vuille, and A. C. Clement (2003), The climate of the Altiplano: Observed current conditions and mechanisms of past changes, *Palaeogeogr. Palaeoclimatol. Palaeoecol.*, *194*, 5–22, doi:10.1016/S0031-0182(03)00269-4.
- Garreaud, R. D., M. Vuille, R. H. Compagnucci, and J. Marengo (2008), Present-day South American climate, *Palaeogeogr. Palaeoclimatol. Palaeoecol.*, in press.
- Giorgi, F., and X. Bi (2005), Regional changes in surface climate interannual variability for the 21st century from ensembles of global model simulations, *Geophys. Res. Lett.*, *32*, L13701, doi:10.1029/2005GL023002.
- Greene, A., R. Seager, and W. Broecker (2002), Tropical snowline depression at the Last Glacial Maximum: Comparison with proxy records using a single-cell tropical climate model, *J. Geophys. Res.*, *107*(D8), 4061, doi:10.1029/2001JD000670.
- Jones, R. G., M. Noguier, D. Hassell, D. Hudson, S. Wilson, G. Jenkins, and J. Mitchell (2004), *Generating High Resolution Climate Change Scenarios Using PRECIS*, 40 pp., Met Office Hadley Cent., Exeter, U.K.
- Jordan, E., L. Ungerechts, B. Cáceres, A. Penafiel, and B. Francou (2005), Estimation by photogrammetry of the glacier recession on the Cotopaxi volcano (Ecuador) between 1956 and 1997, *Hydrol. Sci. J.*, *50*(6), 949–961, doi:10.1623/hysj.2005.50.6.949.
- Juen, I., G. Kaser, and C. Georges (2007), Modeling observed and future runoff from a glacierized tropical catchment (Cordillera Blanca, Perú), *Global Planet. Change*, *59*(1–4), 37–48, doi:10.1016/j.gloplacha.2006.11.038.
- Karmalkar, A. V., R. S. Bradley, and H. F. Diaz (2008), Climate change scenario for Costa Rican montane forests, *Geophys. Res. Lett.*, *35*, L11702, doi:10.1029/2008GL033940.
- Kaser, G., I. Juen, C. Georges, J. Gomez, and W. Tamayo (2003), The impact of glaciers on the runoff and the reconstruction of mass balance history from hydrological data in the tropical Cordillera Blanca, Peru, *J. Hydrol.*, *282*(1–4), 130–144, doi:10.1016/S0022-1694(03)00259-2.
- Lenters, J. D., and K. H. Cook (1997), On the origin of the Bolivian High and related circulation features of the South American climate, *J. Atmos. Sci.*, *54*, 656–677, doi:10.1175/1520-0469(1997)054<0656:OTOOTB>2.0.CO;2.
- Li, W., R. Fu, and R. E. Dickinson (2006), Rainfall and its seasonality over the Amazon in the 21st century as assessed by the coupled models for the IPCC AR4, *J. Geophys. Res.*, *111*, D02111, doi:10.1029/2005JD006355.
- Liebmann, B., J. A. Marengo, J. D. Glick, V. E. Kousky, I. C. Wainer, and O. Massambani (1998), A comparison of rainfall, outgoing longwave radiation and divergence over the Amazon basin, *J. Clim.*, *11*, 2898–2909, doi:10.1175/1520-0442(1998)011<2898:ACOROL>2.0.CO;2.
- Mark, B. G., and J. M. McKenzie (2007), Tracing increasing tropical Andean glacier melt with stable isotopes in water, *Environ. Sci. Technol.*, *41*, 6955–6960, doi:10.1021/es071099d.
- Mark, B. G., and G. O. Seltzer (2005), Evaluation of recent glacier recession in the Cordillera Blanca, Peru (AD 1962–1999), Spatial distribution of mass loss and climatic forcing, *Quat. Sci. Rev.*, *24*, 2265–2280, doi:10.1016/j.quascirev.2005.01.003.
- Mitchell, T. D., and P. D. Jones (2005), An improved method of constructing a database of monthly climate observations and associated high-resolution grids, *Int. J. Climatol.*, *25*, 693–712, doi:10.1002/joc.1181.
- Nakicenovic, N., and R. Swart (Eds.) (2000), *Special Report on Emissions Scenarios*, Cambridge Univ. Press, Cambridge, U.K.
- Nazrul Islam, M., M. Rafiuddin, A. U. Ahmed, and R. K. Kolli (2008), Calibration of PRECIS in employing future scenarios in Bangladesh, *Int. J. Climatol.*, *28*, 617–628, doi:10.1002/joc.1559.
- Pope, V. D., J. A. Pamment, D. R. Jackson, and A. Slingo (2001), The representation of water vapor and its dependence on vertical resolution in the Hadley Centre climate model, *J. Clim.*, *14*, 3065–3085, doi:10.1175/1520-0442(2001)014<3065:TROWVA>2.0.CO;2.
- Ramirez, E., B. Francou, P. Ribstein, M. Desclotres, R. Guérin, J. Mendoza, R. Gallaire, B. Pouyaud, and E. Jordan (2001), Small glaciers disappearing in the tropical Andes: A case study in Bolivia: Glaciar Chacaltaya (16°S), *J. Glaciol.*, *47*(157), 187–194, doi:10.3189/172756501781832214.
- Rauscher, S. A., A. Seth, J.-H. Qian, and S. J. Camargo (2006), Domain choice in a nested modeling prediction system for South America, *Theor. Appl. Climatol.*, *86*, 229–246, doi:10.1007/s00704-006-0206-z.
- Rauscher, S., A. Seth, B. Liebmann, J. Qian, and S. Camargo (2007), Regional climate model—Simulated timing and character of seasonal rains in South America, *Mon. Weather Rev.*, *135*, 2642–2657, doi:10.1175/MWR3424.1.
- Rayner, N. A., D. E. Parker, E. B. Horton, C. K. Folland, L. V. Alexander, D. P. Rowell, E. C. Kent, and A. Kaplan (2003), Global analyses of sea surface temperature, sea ice, and night marine air temperature since the late nineteenth century, *J. Geophys. Res.*, *108*(D14), 4407, doi:10.1029/2002JD002670.

- Roads, J., S. Chen, S. Cocks, L. Druryan, M. Fulakeza, T. LaRow, P. Loneragan, J. Qian, and S. Zebiak (2003), International Research Institute/Applied Research Centers (IRI/ARCs) regional model intercomparison over South America, *J. Geophys. Res.*, 108(D14), 4425, doi:10.1029/2002JD003201.
- Rojas, M. (2006), Multiply nested regional climate simulation for southern South America: Sensitivity to model resolution, *Mon. Weather Rev.*, 134, 2208–2223, doi:10.1175/MWR3167.1.
- Rojas, M., and A. Seth (2003), Simulation and sensitivity in a nested modeling system for South America. Part II: GCM boundary forcing, *J. Clim.*, 16, 2454–2471, doi:10.1175/1520-0442(2003)016<2454:SASIAN>2.0.CO;2.
- Salzmann, N., C. Frei, P. Vidale, and M. Hoelzle (2007), The application of regional climate model output for the simulation of high-mountain permafrost scenarios, *Global Planet. Change*, 56(1–2), 188–202, doi:10.1016/j.gloplacha.2006.07.006.
- Seimon, T. A., A. Seimon, P. Daszak, S. R. P. Halloy, L. M. Schloegel, C. A. Aguiar, P. Sowell, A. D. Hyatt, B. Konecky, and J. E. Simmons (2007), Upward range extension of Andean anurans and chytridiomycosis to extreme elevations in response to tropical deglaciation, *Global Change Biol.*, 13, 288–299, doi:10.1111/j.1365-2486.2006.01278.x.
- Seth, A., and M. Rojas (2003), Simulation and sensitivity in a nested modeling system for South America. Part I: Reanalyses boundary forcing, *J. Clim.*, 16, 2437–2453, doi:10.1175/1520-0442(2003)016<2437:SASIAN>2.0.CO;2.
- Seth, A., M. Rojas, B. Liebmann, and J.-H. Qian (2004), Daily rainfall analysis for South America from a regional climate model and station observations, *Geophys. Res. Lett.*, 31, L07213, doi:10.1029/2003GL019220.
- Seth, A., S. A. Rauscher, S. J. Camargo, J.-H. Qian, and J. S. Pal (2007), RegCM3 regional climatologies for South America using reanalysis and ECHAM global model driving fields, *Clim. Dyn.*, 28, 461–480, doi:10.1007/s00382-006-0191.
- Thompson, L. G., E. Mosley-Thompson, H. Brecher, M. Davis, B. Leon, D. Les, P.-N. Lin, T. Mashiotto, and K. Mountain (2006), Abrupt tropical climate change: Past and present, *Proc. Natl. Acad. Sci. U.S.A.*, 103(28), 10,536–10,543, doi:10.1073/pnas.0603900103.
- Urrutia, R. (2008), Assessment of 21st century climate change projections in tropical South America and the tropical Andes, M.S thesis, 144 pp., Univ. of Mass.-Amherst, Amherst. (Available at <http://www.geo.umass.edu/climate/theses/urrutia-thesis.pdf>)
- Vera, C., G. Silvestri, B. Liebmann, and P. Gonzalez (2006), Climate change scenarios for seasonal precipitation in South America from IPCC-AR4 models, *Geophys. Res. Lett.*, 33, L13707, doi:10.1029/2006GL025759.
- Vergara, W., A. Deeb, A. Valencia, R. Bradley, B. Francou, A. Zarzar, A. Grünwaldt, and S. Haussling (2007), Economic impacts of rapid glacier retreat in the Andes, *Eos Trans. AGU*, 88(25), 261–264, doi:10.1029/2007EO250001.
- Viviroli, D., H. H. Duerr, B. Messerli, M. Meybeck, and R. Weingartner (2007), Mountains of the world, water towers for humanity: Typology, mapping and global significance, *Water Resour. Res.*, 43, W07447, doi:10.1029/2006WR005653.
- Vuille, M. (1999), Atmospheric circulation over the Bolivian Altiplano during dry and wet periods and extreme phases of the Southern Oscillation, *Int. J. Climatol.*, 19, 1579–1600, doi:10.1002/(SICI)1097-0088(19991130)19:14<1579::AID-JOC441>3.0.CO;2-N.
- Vuille, M., and R. S. Bradley (2000), Mean annual temperature trends and their vertical structure in the tropical Andes, *Geophys. Res. Lett.*, 27, 3885–3888, doi:10.1029/2000GL011871.
- Vuille, M., and F. Keimig (2004), Interannual variability of summertime convective cloudiness and precipitation in the central Andes derived from ISCCP-B3 data, *J. Clim.*, 17, 3334–3348, doi:10.1175/1520-0442(2004)017<3334:IVOSCC>2.0.CO;2.
- Vuille, M., R. S. Bradley, and F. Keimig (2000a), Climate variability in the Andes of Ecuador and its relation to tropical Pacific and Atlantic sea surface temperatures anomalies, *J. Clim.*, 13, 2520–2535, doi:10.1175/1520-0442(2000)013<2520:CVITAO>2.0.CO;2.
- Vuille, M., R. S. Bradley, and F. Keimig (2000b), Interannual climate variability in the central Andes and its relation to tropical Pacific and Atlantic forcing, *J. Geophys. Res.*, 105, 12,447–12,460, doi:10.1029/2000JD900134.
- Vuille, M., R. Bradley, M. Werner, and F. Keimig (2003), 20th century climate change in the tropical Andes: Observations and model results, *Clim. Change*, 59(1–2), 75–99, doi:10.1023/A:1024406427519.
- Vuille, M., B. Francou, P. Wagnon, I. Juen, G. Kaser, B. G. Mark, and R. S. Bradley (2008a), Climate change and tropical Andean glaciers—Past, present and future, *Earth Sci. Rev.*, 89, 79–96, doi:10.1016/j.earscirev.2008.04.002.
- Vuille, M., G. Kaser, and I. Juen (2008b), Glacier mass balance variability in the Cordillera Blanca, Peru and its relationship with climate and the large scale circulation, *Global Planet. Change*, 62(1–2), 14–28, doi:10.1016/j.gloplacha.2007.11.003.
- Xie, P., and P. A. Arkin (1997), Global precipitation: A 17-year monthly analysis based on gauge observations, satellite estimates, and numerical model outputs, *Bull. Am. Meteorol. Soc.*, 78, 2539–2558, doi:10.1175/1520-0477(1997)078<2539:GPAYMA>2.0.CO;2.
- Young, K. R., and J. K. Lipton (2006), Adaptive governance and climate change in the tropical highlands of western South America, *Clim. Change*, 78, 63–102, doi:10.1007/s10584-006-9091-9.
- Zhang, Y., Y. Xu, W. Dong, L. Cao, and M. Sparrow (2006), A future scenario of regional changes in extreme climate events over China using the PRECIS climate model, *Geophys. Res. Lett.*, 33, L24702, doi:10.1029/2006GL027229.

R. Urrutia, Laboratorio de Dendrocronología, Instituto de Silvicultura, Universidad Austral de Chile, Independencia 641 Valdivia, Chile. (rociourrutia@uach.cl)

M. Vuille, Department of Earth and Atmospheric Science, State University of New York at Albany, 1400 Washington Avenue, Albany, NY 12222, USA. (mathias@atmos.albany.edu)